

Corrigendum to “Binder-free nanostructured germanium anode for high resilience lithium-ion battery”



S. Fugattini ^{a,b,c,†,*}, U. Gulzar ^{b,†}, A. Andreoli ^{a,†}, L. Carbone ^{b,*}, M. Boschetti ^a, P. Bernardoni ^a, M. Gjestila ^a, G. Mangherini ^a, R. Camattari ^{a,f}, T. Li ^b, S. Monaco ^{b,*}, M. Ricci ^b, S. Liang ^b, D. Giubertoni ^c, G. Pepponi ^c, P. Bellutti ^c, M. Ferroni ^{d,e}, L. Ortolani ^e, V. Morandi ^e, D. Vincenzi ^{a,*}, R. Proietti Zaccaria ^{b,g,*}

^a University of Ferrara, Physics and Earth Sciences Department via Saragat 1, 44122 Ferrara, Italy

^b Italian Institute of Technology, via Morego 30, 16163 Genova (GE), Italy

^c Bruno Kessler Foundation, via Sommarive, 18 38123 Povo (TN), Italy

^d Department of Civil, Environmental, Architectural Engineering and Mathematics, University of Brescia - Via Valotti, 9 - 25123 Brescia

^e CNR-IMM Bologna Section, Via Gobetti, 101 - 40129 Bologna, Italy

^f National Institute of Nuclear Physics (INFN) - section of Ferrara, via Saragat 1, 44122 Ferrara, Italy

^g Cixi Institute of Biomedical Engineering, Ningbo Institute of Materials Technology and Engineering, Chinese Academy of Sciences, Zhejiang 315201, PR China

The authors have included all the figures of the main text and of the supplementary information in high resolution along with Table 1 properly aligned here. Figs. 1–7 and Fig. S1–S5.

DOI of original article: <https://doi.org/10.1016/j.electacta.2022.139832>.

* Corresponding authors.

E-mail addresses: silvio.fugattini@gmail.com (S. Fugattini), Lorenzo.Carbone@lithium.plus (L. Carbone), monaco.simone@alice.it (S. Monaco), donato.vincenzi@unife.it (D. Vincenzi), remo.proietti@iit.it (R. Proietti Zaccaria).

† These authors contributed equally to this study.

Table 1
Performance comparison of Ge-based anode materials from literature.

Material	Preparation method	Specific capacity [mAh g ⁻¹] (low C-rate)	Specific capacity [mAh g ⁻¹] (high C-rate)	Overall number of cycles (C-rate, spec. cap. [mAh g ⁻¹])	Mass loading [mg] (mass density [mg/ cm ²])	Ge content [%]	Voltage range [V]	Ref.
Nanostructured Ge film	PECVD + HF etching	1250 (0.1C)	450 (60C)	2500 (1C, 925)	0.2-0.3 (0.11- 0.17)	100	0.01 - 1.5	This work [1]
Sn-seeded nanowires	Vapor-Liquid-Solid (VLS) technique	1250 (0.1C)	722 (2C)	1100 (0.5C, 888)	— (0.22)	83 (5:1 ratio Ge:Sn)	0.01 - 1.5	[2]
Amorphous Ge films	Physical Vapor Deposition (PVD)	1700 (C/4)	500 (1000C charge, 1C discharge)	60 (C/4, 1700)	0.042 (—)	100	0 - 1.5	[3]
Ge grains	Thermal reduction of GeO ₂	1500 (C/30)	1100 (0.5C)	40 (0.5C, 1100)	—	—	0.02 - 2.0	[4]
Ge nanowires	Thermal co- evaporation method	—	900 (1C)	50 (1C, 900)	—	—	0 - 1.2	[5]
Ge nanowires	VLS technique	1141 (C/20)	600 (2C)	50 (rate cap., 600)	1.0 (—)	~ 100	0 - 2.5	[6]
Ge nanowires	Vapor-solid-solid mechanism	1318 (0.1C)	1081 (2C)	1900 (1C, 866)	— (0.19)	~ 100	0.01 - 1.5	[7]
Ge nanowires in graphite tubes	CVD system	1310 (C/6)	232 (6C)	110 (rate cap., 1300)	0.5 (—)	70 (Ge- graphite)	0.005 - 1.2	[8]
Ge nanowires	VLS technique	1405 (0.1C)	1200 (5C)	100 (rate cap., 1200)	0.12-0.86 (—)	~ 100	0.01 - 2.0	[9]
Ge nanotubes	Kirkendall effect	1022 (0.2C)	580 (20C)	50 (0.2C, 1002)	—	—	0 - 1.5	[10]
Ge microcubes	Hydrogen reduction method	1250 (0.1C)	1121 (50C charge, 1C discharge)	500 (1C, 1204)	— (~ 2)	100	0.005 - 1.5	[11]
Ge/SWCNT paper (34% Ge)	Ge particles deposited on SWCNT	750 (0.015C)	—	40 (0.015C, 417)	—	—	0.01 - 2.0	[12]
Micro sized porous Ge particles	Reduction of GeO ₂	1100 (0.6C)	437 (10C)	1800 (5C, 469)	— (0.56-1)	70	0.02 - 1.2	[13]
Ge micro particles	Halogen-free process	600 (1C)	200 (10C)	25 (1C, 580)	0.5-1 (—)	—	0.05 - 1.5	[14]
Ge/Co ₃ O ₄ nano-rod array	Electron beam evaporation	1237 (0.5C)	675 (20C)	600 (10C, 1018)	— (0.19)	100	0.02 - 1.0	[15]
Ge nanoparticles	Chemical de-alloying process	1191 (0.1C)	767 (1C)	210 (rate cap., 1200)	—	—	0.05 - 0.9	[16]
Mesoporous Germanium	Mechanochemical reaction	950 (0.1C)	—	20 (0.1C, 789)	—	—	0 - 1.5	[17]
Ge powder	Commercial Ge powder	1152 (1C)	700 (10C)	2500 (variable C- rates, 1152)	— (0.3-0.5)	40	0 - 1.0	[18]

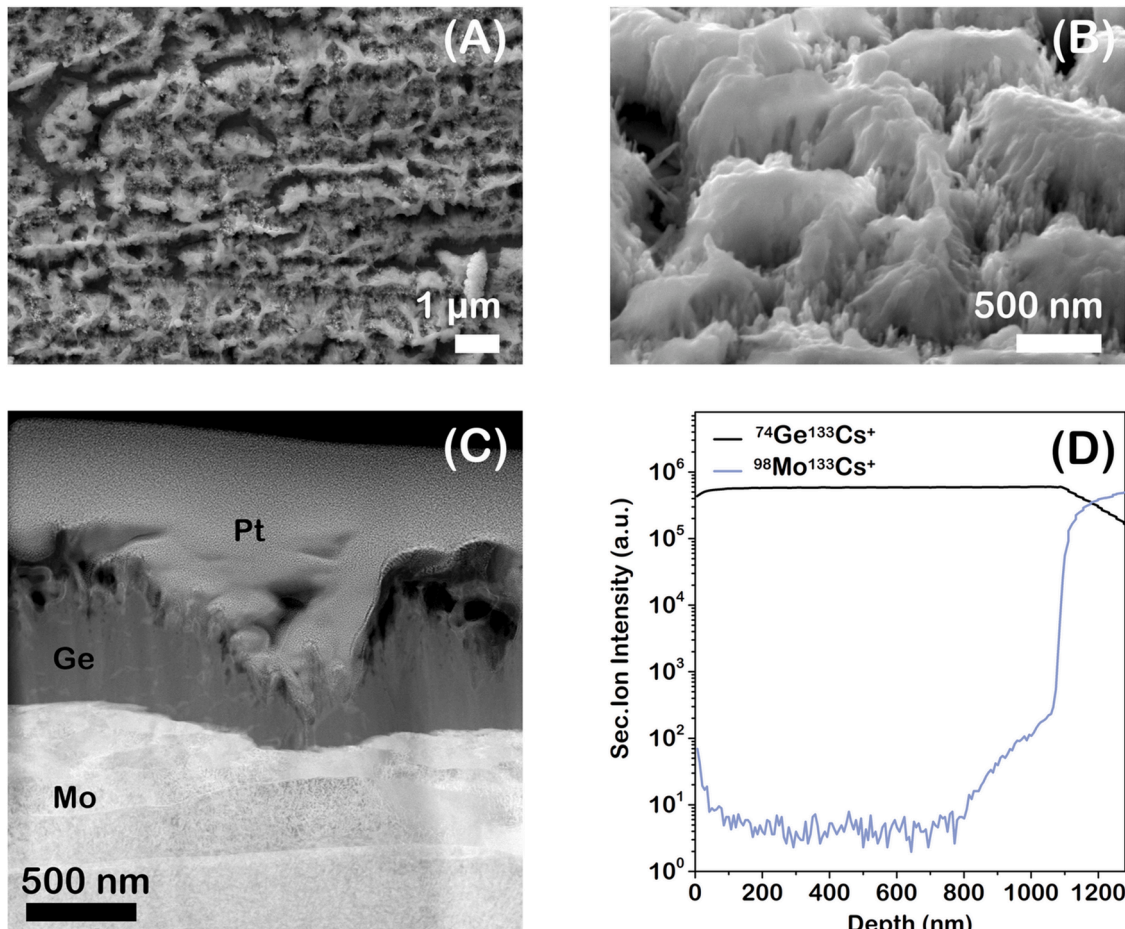


Fig. 1. Top-view (A) and tilted (B) SEM images of the nanostructured Ge film. TEM image (C) of the cross-sectional specimen, Ge and Mo SIMS depth profiles (D) of the as-deposited film.

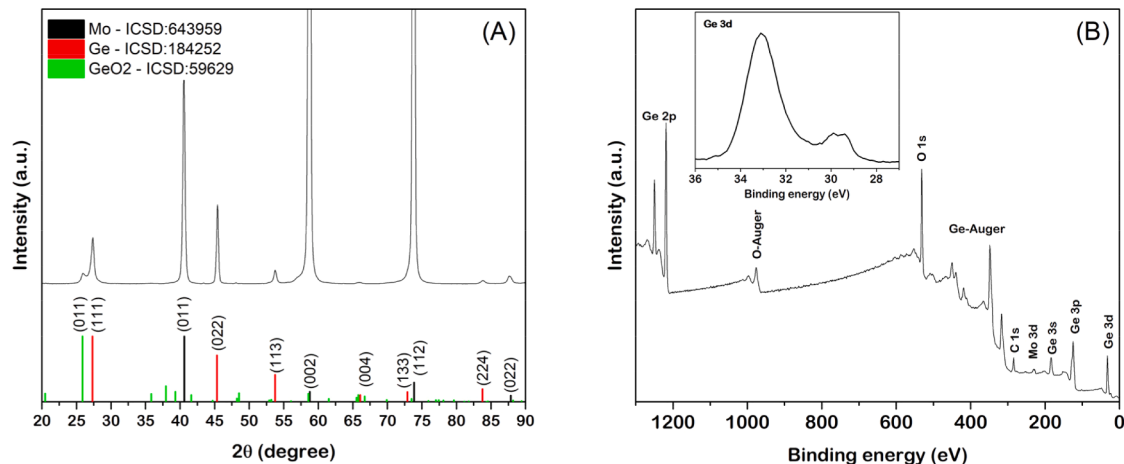


Fig. 2. XRD pattern (A) and XPS wide survey (B) of the nanostructured Ge film. The inset in (B) reports the magnification of the Ge 3d peak.

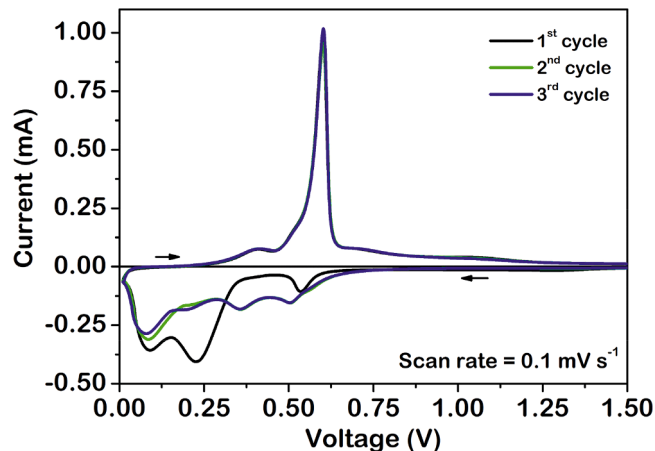


Fig. 3. Cyclic voltammetry of the nanostructured Ge anode performed at 0.1 mV s⁻¹ in the voltage range 0.01–1.5 V. The CV starts from 1.5 V and follows the direction indicated by the arrows.

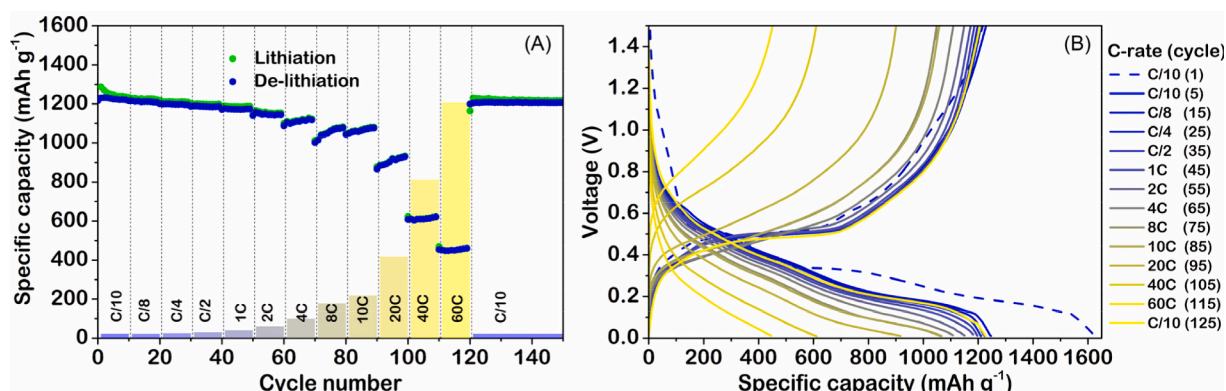


Fig. 4. Rate capability (A) and charge/discharge profiles (B) of the nanostructured Ge anode performed at various C-rates (from C/10 up to 60C) in the 0.01–1.5 V voltage range, changing the current rate every 10 cycles. The dashed line in (B) is the first charge/discharge profile.

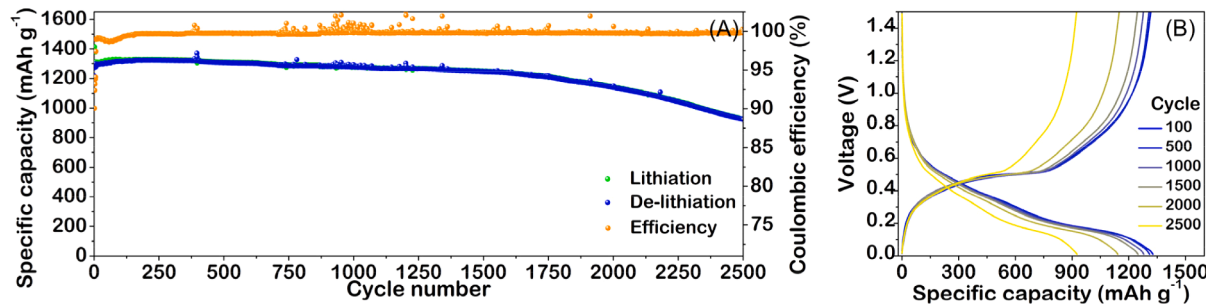


Fig. 5. Long cycling behaviour (A) and charge/discharge profiles (B) of the nanostructured Ge anode at the current rate of 1C in the 0.01–1.5 V voltage range.

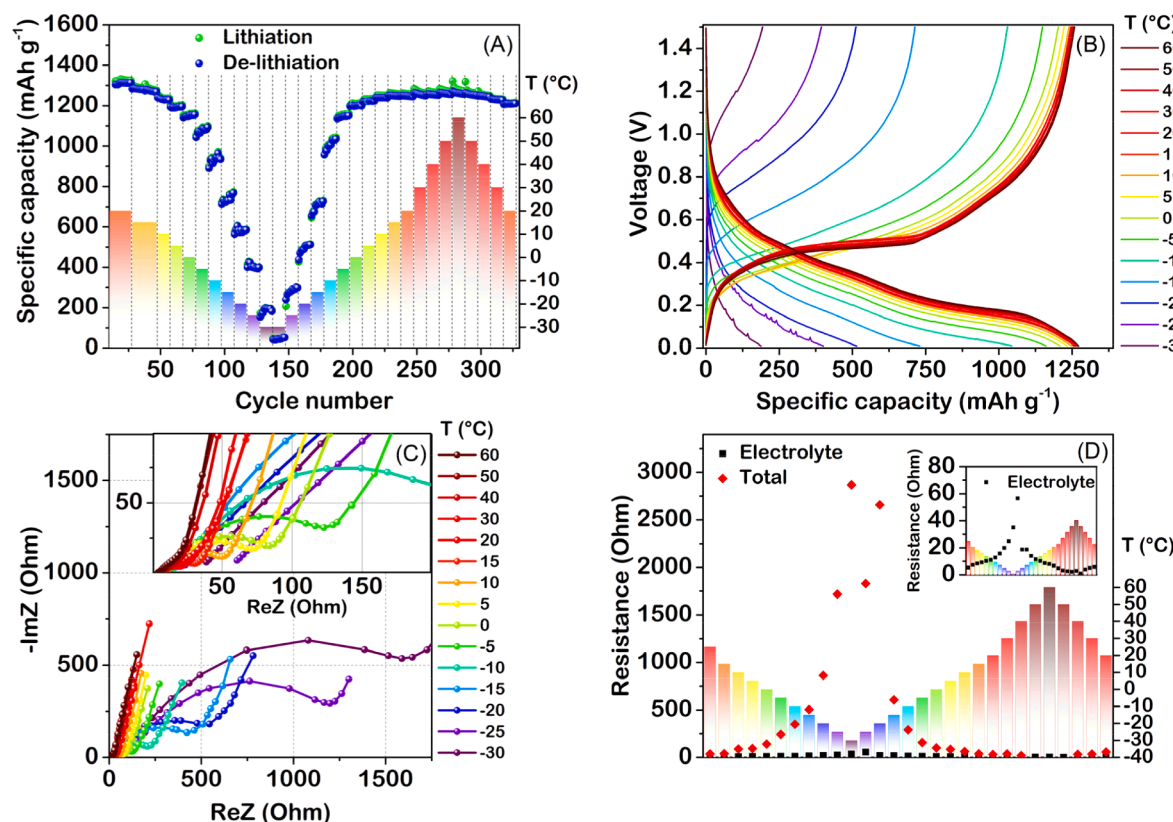


Fig. 6. Specific capacity versus cycle number (A) and charge/discharge profiles (B) of the nanostructured Ge anode performed at the current rate of 1C. The bars in (A) and (D) represent the temperature at which each cycle is performed that varies every 10 cycles from RT to -30°C, heating up to +60°C and finally back to RT. In (C) Nyquist plots of the impedance spectroscopy tests performed every temperature step in the 0.1 Hz–10 kHz frequency range. Electrolyte and total resistance values are extrapolated fitting the Nyquist plots and represented versus the temperature (D).

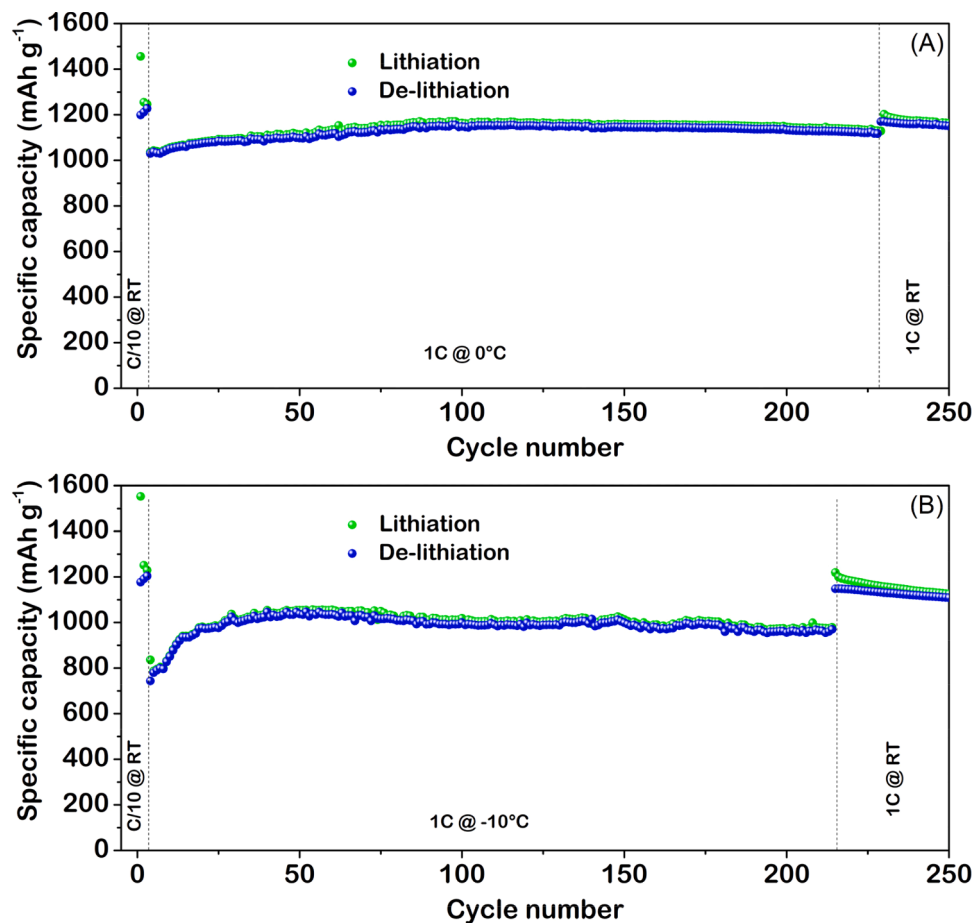


Fig. 7. Long cycling behaviour of the nanostructured Ge anode at the current rate of 1C in the 0.01–1.5 V voltage range at 0°C (A) and -10°C (B).

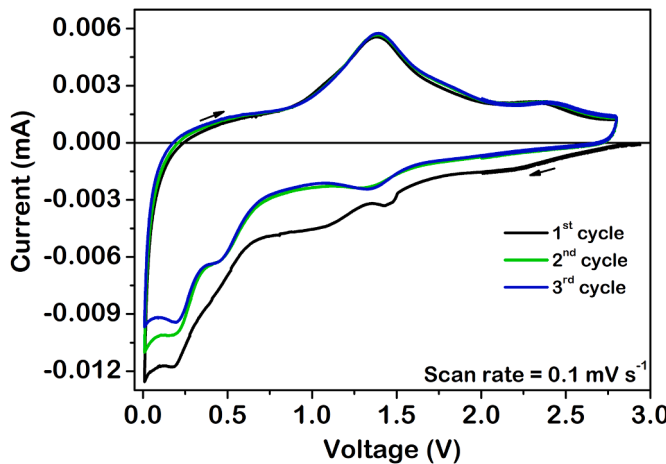


Fig. S1. Cyclic voltammetry of a bare Mo foil as anode performed at 0.1 mV s⁻¹ in the voltage range 0.01–2.8 V.

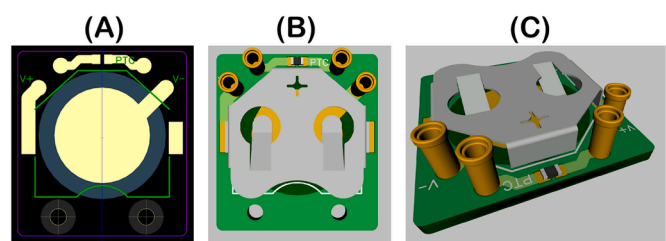


Fig. S2. PCB designed for testing a 2032 coin-cell inside the OXFORD cryostat CCC1204: scheme (A), plan (B) and oblique (C) rendering. Two wires were soldered on each of the V+ and V- pins, to allow a four contact measurement of the cell voltage/current. In the top part of the scheme (A) the two contacts for the temperature sensor (Pt1000) are clearly visible. In the two rendered images (B-C) the coin-cell holder, the Pt1000 sensor, and the four-wire connections are depicted.

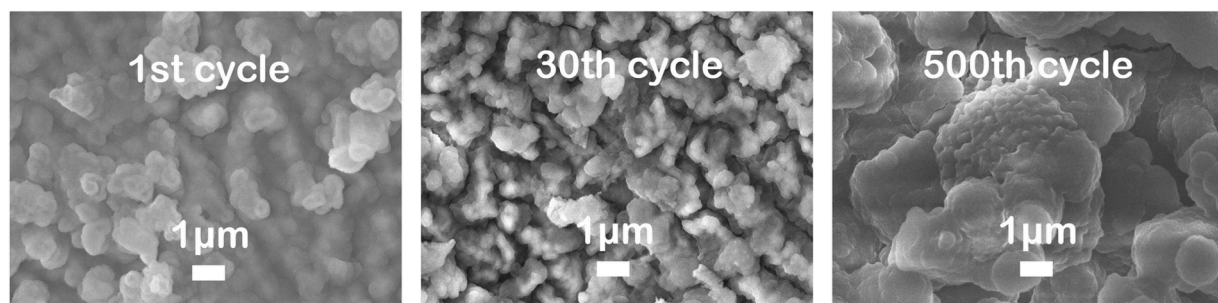


Fig. S3. SEM top-view pictures of the nanostructured Ge electrode after the 1st, the 30th and at the 500th cycle.

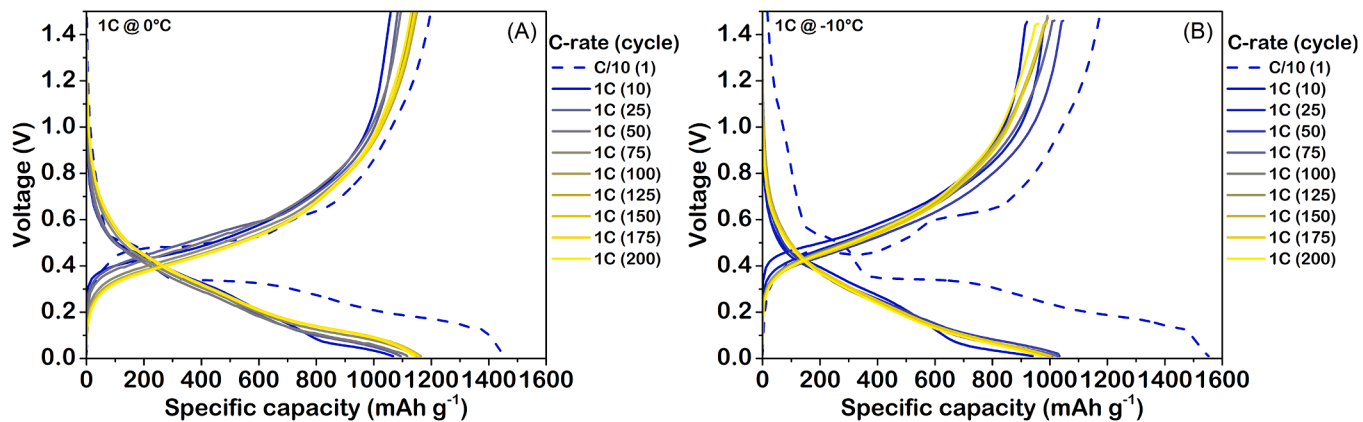


Fig. S4. Charge/discharge profiles of the nanostructured Ge anode performed at the current rate of 1C at 0°C (A) and -10°C (B).

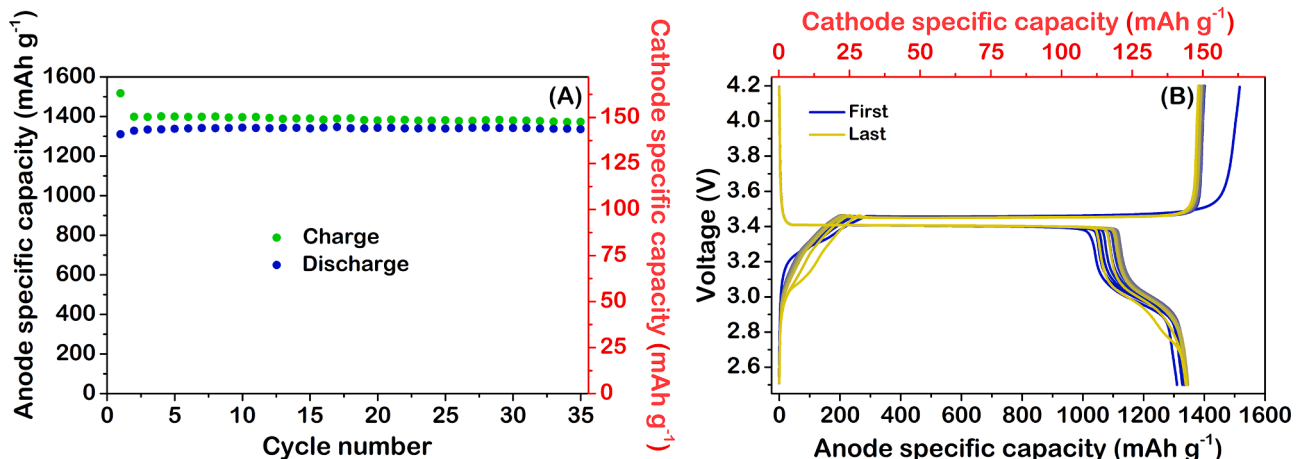


Fig. S5. Cycling behaviour (A) and charge/discharge profiles (B) of the full-cell realized by coupling the nanostructured Ge anode and the LiFePO₄ cathode at the current rate of C/10 in the 2.5–4.2 V voltage range. In both graphs the specific capacity of the cell is reported considering the anode (in black) and the cathode (in red) active mass.

References

- [1] S. Fugattini, U. Gulzar, A. Andreoli, L. Carbone, M. Boschetti, P. Bernardoni, M. Gjestila, G. Mangherini, R. Camattari, T. Li, S. Monaco, M. Ricci, S. Liang, D. Giubertoni, G. Pepponi, P. Bellutti, M. Ferroni, L. Ortolani, V. Morandi, D. Vincenzi, R.P. Zaccaria, Binder-free nanostructured germanium anode for high resilience lithium-ion battery, *Electrochim. Acta* (2022), 139832, <https://doi.org/10.1016/J.ELECTACTA.2022.139832>.
- [2] T. Kennedy, E. Mullane, H. Geaney, M. Osiak, C. O'Dwyer, K.M. Ryan, High-performance germanium nanowire-based lithium-ion battery anodes extending over 1000 cycles through *in situ* formation of a continuous porous network, *Nano Lett.* 14 (2014) 716–723, <https://doi.org/10.1021/nl403979s>.
- [3] J. Graetz, C.C. Ahn, R. Yazami, B. Fultz, Nanocrystalline and thin film germanium electrodes with high lithium capacity and high rate capabilities, *J. Electrochem. Soc.* 151 (2004) 698–702, <https://doi.org/10.1149/1.1697412>.
- [4] F.S. Ke, K. Mishra, L. Jamison, X.X. Peng, S.G. Ma, L. Huang, S.G. Sun, X.D. Zhou, Tailoring nanostructures in micrometer size germanium particles to improve their performance as an anode for lithium ion batteries, *Chem. Commun.* 50 (2014) 3713–3715, <https://doi.org/10.1039/c4cc00051j>.
- [5] Y.D. Ko, J.G. Kang, G.H. Lee, J.G. Park, K.S. Park, Y.H. Jin, D.W. Kim, Sn-induced low-temperature growth of Ge nanowire electrodes with a large lithium storage capacity, *Nanoscale* 3 (2011) 3371–3375, <https://doi.org/10.1039/c1nr10471c>.
- [6] C.K. Chan, X.F. Zhang, Y. Cui, High capacity Li ion battery anodes using Ge nanowires, *Nano Lett.* 8 (2008) 307–309, <https://doi.org/10.1021/nl0727157>.
- [7] E. Mullane, T. Kennedy, H. Geaney, K.M. Ryan, A rapid, solvent-free protocol for the synthesis of germanium nanowire lithium-ion anodes with a long cycle life and high rate capability, *ACS Appl. Mater. Interfaces*. 6 (2014) 18800–18807, <https://doi.org/10.1021/am5045168>.
- [8] Y. Sun, S. Jin, G. Yang, J. Wang, C. Wang, Germanium Nanowires-in-Graphite Tubes via Self-Catalyzed Synergetic Confined Growth and Shell-Splitting Enhanced

- Li-Storage Performance, ACS Nano 9 (2015) 3479–3490, <https://doi.org/10.1021/nn506955f>.
- [9] B. Farbod, K. Cui, M. Kupsta, W.P. Kalisvaart, E. Memarzadeh, A. Kohandehghan, B. Zahiri, D. Mitlin, Array geometry dictates electrochemical performance of Ge nanowire lithium ion battery anodes, J. Mater. Chem. A. 2 (2014) 16770–16785, <https://doi.org/10.1039/c4ta03805c>.
- [10] M.H. Park, Y. Cho, K. Kim, J. Kim, M. Liu, J. Cho, Germanium nanotubes prepared by using the Kirkendall effect as anodes for high-rate lithium batteries, Angew. Chemie - Int. Ed. 50 (2011) 9647–9650, <https://doi.org/10.1002/anie.201103062>.
- [11] C. Zhang, Z. Lin, Z. Yang, D. Xiao, P. Hu, H. Xu, Y. Duan, S. Pang, L. Gu, G. Cui, Hierarchically designed germanium microcubes with high initial coulombic efficiency toward highly reversible lithium storage, Chem. Mater. 27 (2015) 2189–2194, <https://doi.org/10.1021/acs.chemmater.5b00218>.
- [12] J. Wang, J.Z. Wang, Z.Q. Sun, X.W. Gao, C. Zhong, S.L. Chou, H.K. Liu, A germanium/single-walled carbon nanotube composite paper as a free-standing anode for lithium-ion batteries, J. Mater. Chem. A. 2 (2014) 4613–4618, <https://doi.org/10.1039/c3ta14934j>.
- [13] K. Mishra, X.C. Liu, F.S. Ke, X.D. Zhou, Porous germanium enabled high areal capacity anode for lithium-ion batteries, Compos. Part B Eng. (2019), <https://doi.org/10.1016/j.compositesb.2018.10.076>.
- [14] E.A. Saverina, V. Sivasankaran, R.R. Kapaev, A.S. Galushko, V.P. Ananikov, M. P. Egorov, V.V. Joukov, P.A. Troshin, M.A. Syroeshkin, An environment-friendly approach to produce nanostructured germanium anodes for lithium-ion batteries, Green Chem. (2020), <https://doi.org/10.1039/c9gc02348h>.
- [15] X. Li, Z. Yang, Y. Fu, L. Qiao, D. Li, H. Yue, D. He, Germanium anode with excellent lithium storage performance in a germanium/lithium-cobalt oxide lithium-ion battery, ACS Nano 9 (2015) 1858–1867, <https://doi.org/10.1021/nn506760p>.
- [16] S. Liu, J. Feng, X. Bian, Y. Qian, J. Liu, H. Xu, Nanoporous germanium as high-capacity lithium-ion battery anode, Nano Energy 13 (2015) 651–657, <https://doi.org/10.1016/j.nanoen.2015.03.039>.
- [17] L.C. Yang, Q.S. Gao, L. Li, Y. Tang, Y.P. Wu, Mesoporous germanium as anode material of high capacity and good cycling prepared by a mechanochemical reaction, Electrochim. Commun. (2010), <https://doi.org/10.1016/j.elecom.2010.01.008>.
- [18] K.C. Klavetter, S.M. Wood, Y.M. Lin, J.L. Snider, N.C. Davy, A.M. Chockla, D. K. Romanovicz, B.A. Korgel, J.W. Lee, A. Heller, C.B. Mullins, A high-rate germanium-particle slurry cast Li-ion anode with high Coulombic efficiency and long cycle life, J. Power Sources. (2013), <https://doi.org/10.1016/j.jpowsour.2013.02.091>.